International Journal of
Plasma Environmental Science and Technology

Regular Paper DOI: 10.34343/ijpest.2023.17.e01006

Reduction of CCl_2F_2 emission via plasma catalysis

Shin Wen[1], Kuan Lun Pan[2], Amir Machmud[1], Moo Been Chang[1],*

[1] Graduate Institute of Environmental Engineering, National Central University, Taiwan
[2] Green Energy and Environmental Institute, Industrial Technology Research Institute, Hsinchu, Taiwan

* Corresponding author: mbchang@ncuen.ncu.edu.tw (Moo Been Chang)

Received: 25 October 2022
Revised: 1 February 2023
Accepted: 22 March 2023
Published online: 29 March 2023

Abstract

Dichlorodifluoromethane (CCl_2F_2/CFC-12) is widely used as refrigerant, foaming agent and aerosol propellant in industry. Due to its chemical stability, CCl_2F_2 gradually diffuses from the troposphere to the stratosphere once released and catalyzes the destruction of ozone through photodegradation. In addition, CCl_2F_2 is listed as a potent greenhouse gas with a high global warming potential (GWP = 10.2). Current technologies for treating CCl_2F_2 include combustion, catalysis, and plasma destruction. This study aims to develop a catalyst with good activity and integrate it with plasma to form a hybrid system for the removal of CCl_2F_2 from gas streams. The results obtained show that combined plasma with catalyst (plasma catalysis system) is effective in removing CCl_2F_2 and the highest removal efficiency of 99.0% is achieved for the operating conditions of applied voltage 17 kV, gas flow rate 500 sccm, [CCl_2F_2] = 800 ppm and [O_2] =1%. Nitrogen atoms, excited N_2 molecules such as $N_2(A^3\sum_u^+)$ $N^*(^4S, ^2D, ^2P)$ and high-energy electrons generated by plasma are beneficial for the removal mechanism of CFC-12. In the presence of oxygen, the main byproducts of CCl_2F_2 conversion include CO_2, $CClF_3$, N_2O and NO_X. This study confirms that addition of Mn into TiO_2 greatly improves the removal efficiency of CCl_2F_2 and this system has good potential for industrial application.

Keywords: CCl_2F_2, global warming, ozone depleting substances, plasma catalysis.

1. Introduction

Refrigerants are essential in air-conditioning, coolers, pre-coolers, refrigerators, heat pumps, and freezers to maintain a specific temperature or cooling. Material used as refrigerant should own a high heat absorption capacity and thermal stability. Halogen-containing compounds such as chlorofluorocarbons (CFCs) are commonly used in industrial activities and daily life as a refrigerant material [1].

CFCs were first developed in the early 1930s [1]. Due to their low toxicity, non-flammability, low thermal conductivity, good chemical stability, low corrosives, and reasonable price [2], CFCs have been widely used as refrigerants, solvents, propellants and foaming agents. One of the examples is the utilization of trichlorofluoromethane (CCl_3F/CFC-11) in aerosol propellant mixtures. However, its function had been gradually replaced by other substances after 1990 [3]. Dichlorodifluoromethane (CCl_2F_2/CFC-12) was developed as a refrigerant in the 1930s. It was also often used as aerosol propellant [4]. Despite of the vast application of CCl_2F_2, it is also one the most dangerous threats for ozone layer. CCl_2F_2 has a considerably high global warming potential (GWP) of 10.2 and ozone depleting potential (ODP) of 1 [5–6].

CFCs can drift upwards towards the stratosphere where CFCs are easy to break up by ultraviolet radiation to generate Cl atoms [7]. Cl atom generated would participate in the formation of ClO_x when in contact with the ozone layer, leading to the destruction of ozone molecules and weakening the ozone layer's capability to filter out harmful ultraviolet light. In 1987, many countries signed the Montreal Protocol on substances that deplete the ozone layer. The aim is to avoid the continued damage and deterioration of chlorofluorocarbons to the earth's ozone layer by controlling the production and usage of CFCs, halons and relevant substances [1].

The technologies available for abatement chlorofluorocarbons include combustion, adsorption, catalysis, and thermal plasma technology [8–10]. However, these methods have certain drawbacks such as high fuel cost of combustion, limited adsorption capacity, and catalyst poisoning of the thermal catalysis. Thus, it is essential

to develop an efficient method to degrade CCl_2F_2. As an innovative technology, plasma catalysis has been studied in recent years for dry reforming of methane, syngas production, hydrogen production, methanation, and ammonia (NH_3) synthesis [11–13]. Recently, several researchers investigated the decomposition of CCl_2F_2 over metal oxide catalysts including Al_2O_3, TiO_2, zeolites, and ZrO_2 [14–17]. Researchers have made considerable efforts to utilize TiO_2 as a catalyst in plasma catalysts because it has the following advantages: nontoxic, biocompatible, and inexpensive material with a high dielectric constant and chemical stability [18]. Despite of the numerous advantages, using pure TiO_2 as catalyst might be a shortfall. Wallis *et al*. (2007) reported that utilizing TiO_2 as a catalyst for CCl_2F_2 conversion via plasma catalysis reveals a low destruction efficiency (η = 27) % [14].

According to Kim *et al*. (2007), some of the most important aspects in the oxidation process via plasma catalysis are the influence of oxygen content and loading amount of transition metal in catalyst that plays a key role in the oxidation process [12]. Ogata *et al*. (2005) showed that lattice oxygen from the catalyst plays a role in the oxidation of CCl_2F_2 [16]. Therefore, it is necessary to increase the oxidation state and lattice oxygen of TiO_2 through the addition of a transition metal such as Mn to enhance CCl_2F_2 decomposition efficiency. This research aims to develop an effective Mn/TiO_2 catalyst and to combine it with a plasma system in removing CCl_2F_2. The efficiency and mechanism of the plasma catalysis system to remove CCl_2F_2 by changing the operating parameters are also investigated.

2. Methods

2.1 Catalyst preparation

In this study, impregnation method was used to prepare the catalyst. Mn/TiO_2 catalyst is a mixture of $(Mn(NO_3)_3 \cdot 6H_2O)$ and TiO_2 with a ratio of 10:90 by wt%. The mixture was dissolved in deionized water and the homogeneous solution was stirred at 80 °C until the solution formed a gel. The gel-like sample obtained was placed in an oven and dried at 105 °C for 24 hours. After drying, the gel was placed at a high temperature and heated at a heating rate of 10 °C per minute. The temperature was raised to 500 °C and held for 5 hours. The powder catalyst obtained was denoted as Mn/TiO_2. The Mn/TiO_2 catalyst was ground to the size of 30−70 mesh for the activity tests.

2.2 Experimental setup

The plasma reaction system is a schematically shown in Fig. 1. It consists of a dielectric barrier discharge (DBD) reactor, AC power supply, frequency adjuster, and an oscilloscope. The DBD reactor was made of a quartz tube (inner diameter = 17 mm with gap 7.25 mm) filled with Mn/TiO_2 catalyst place in the discharge zone, which means volume discharge is equal to the volume of catalyst 2.5 cm^3. The gas hourly specific velocity (GHSV) was calculated as 6,000-24,000 h^{-1}. The DBD reactor used in the experiment was a coaxial cylindrical reactor. A stainless-steel rod with a diameter of 3 mm was utilized as a ground electrode. The aluminum foil was fixed with a stainless-steel mesh as a high-voltage electrode. The gas composition was controlled as follows: $[CCl_2F_2]$ = 800-7200 ppm, $[O_2]$ = 0-10%, and N_2 was applied as the carrier gas. The total flow rate of the gas was 500-2,000 sccm. A gas analyzer (Testo 350) was used to monitor the concentrations of NO_x and CO_2 in the simulated flue gas online. The absolute power is calculated using the applied voltage and current shown in the oscilloscope. CCl_2F_2 and byproducts were determined by Fourier transform infrared spectroscopy (FTIR, Nicolet 6700). For the analysis of the experimental results, the conversion efficiency (η) and removal rate (mg h^{-1}) of CCl_2F_2 are calculated by Equations (1) and (2).

$$\eta(\%) = \frac{[CCl_2F_2]_{in} - [CCl_2F_2]_{out}}{[CCl_2F_2]_{in}} \times 100\% \quad (1)$$

$$Removal\ rate(mg/h) = Q \times C_{in} \times \eta(\%) \times \frac{MW}{24.45} \quad (2)$$

where, $[CCl_2F_2]_{in}$ is the inlet CCl_2F_2 concentration, $[CCl_2F_2]_{out}$ is the outlet CCl_2F_2 concentration, Q is total gas flow rate, 24.45 is conversion factor and MW is the molecular weight of CCl_2F_2.

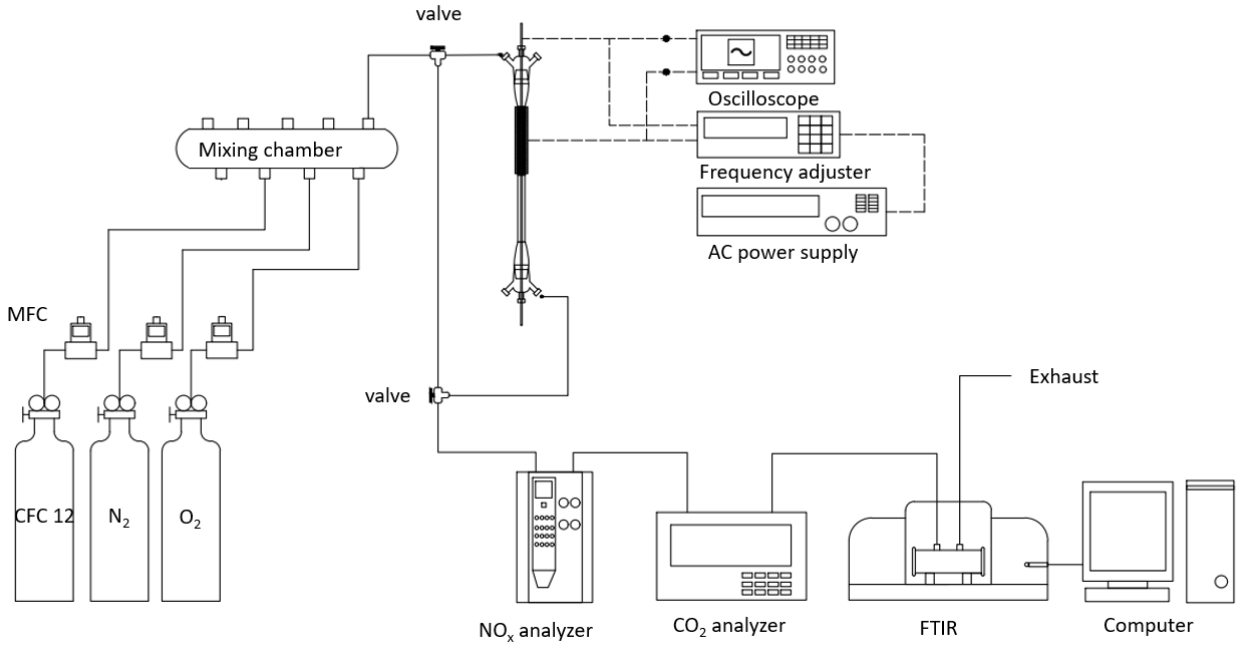

Fig. 1. Schematic of the plasma system.

3. Results and discussion

3.1 Effect of O_2 content on CCl_2F_2 removal

Fig.2 shows the effectiveness of plasma catalysis with Mn/TiO_2 as catalyst for converting CCl_2F_2 at an applied voltage ranging from 13 to17 kV. Gas streams containing 800 ppm CCl_2F_2 with a total gas flow rate of 500 sccm and O_2 content varying from 0 to 10% were generated for experimental tests. As shown in Fig. 2, the removal efficiency of CCl_2F_2 achieved with the system increased gradually with the increase of operating voltage. At 13 kV, the lowest removal efficiency achieved was 9% in the absence of O_2. At 17 kV, the removal efficiency of CCl_2F_2 in the absence of O_2 was the highest, being > 99%. At the same voltage, CCl_2F_2 removal efficiency decreased to 65% as the O_2 content was increased to 10 %. As shown in Fig. 2, adding 1% O_2 to the gas stream reveals a comparatively better CCl_2F_2 removal efficiency. However, excess oxygen results in a significant reduction of CCl_2F_2 conversion. At 13 kV, the removal efficiency of CCl_2F_2 was only 29% when 1% O_2 was added. The increase in CCl_2F_2 conversion with the addition of 1% O_2 can only be seen at the applied voltage of 13-16 kV. At 17 kV, addition of 1% oxygen shows a decrease in the conversion of CCl_2F_2.

Increasing applied voltage could increase the amount of energetic electrons for effective CCl_2F_2 removal. In the absence of oxygen, the conversion of CCl_2F_2 is facilitated by the supply of energetic electrons. In contrast, in the presence of excess oxygen, some energetic electrons would attach to oxygen due to its electronegative properties. This might inhibit the removal of CCl_2F_2. Additionally, a high conversion value is promised by the factors like the applied voltage. However, increasing applied voltage might not guarantee an optimal energy efficiency. A high applied voltage caused a high conversion that is negatively correlated with the energy efficiency [21, 41]. Therefore, it's essential to find appropriate applied voltage in order to maintain a high energy efficiency.

The combination of Mn/TiO_2 catalyst with plasma chemistry leads to efficient CCl_2F_2 removal. Several factors might contribute to this phenomenon, such as: 1) The presence of a catalyst in the discharge zone can extend the residence time. The presence of catalyst would provide numerous active sites for the adsorption of CCl_2F_2 molecules, extending the residence time of CCl_2F_2 in the discharge zone. According to Kim *et al*. (2016) and KP Veerapandian *et al*. (2019), addition of appropriate catalyst can adsorb gas pollutants in a plasma catalysis system [55,56]. These findings demonstrate that catalysts and plasma can interact to enhance the removal of CCl_2F_2. 2) The presence of a Mn/TiO_2 catalyst in the plasma system can increase the electric field. According to Azadmanjiri *et al*. (2014) TiO_2 has a dielectric constant of 95 [44]. Zhang *et al*. (2016)

indicated that dielectric constant is one of the most important factors in plasma generation [45]. The presence of a catalyst with a high dielectric constant can increase the number of contact points, resulting in a significant impact on the electric field (E), mean electric field (Ex), and electron distribution function (EEDF) [21, 24, 43]. 3) TiO_2 has a basic property as a photocatalytic material with a band gap of 3.2 eV and a Schottky defect that results in *n*-type semiconducting properties [48]. On the other hand, TiO_2 has the capacity to absorb UV light at 385 nm, which is followed by electron-hole pair generation, resulting in excess radical cations [14]. Furthermore, Fu *et al.* (2021) found that adding a transition metal, such as Mn, boosts the photocatalytic process [19]. In plasma chemistry, the formation of UV rays in the discharge zone also contributes to this photocatalytic process. Sano *et al*. (2006) explained that photocatalytic processes in plasma catalysis could occur when TiO_2 absorbs UV light ($300 < \lambda < 380$ nm) emitted from N_2 plasma [49]. Due to the aforementioned reasons, we conclude that using Mn/TiO_2 catalyst to combine with plasma chemistry is effective for the removal of CCl_2F_2. 4) The effect of oxygen lattice and oxidation state on Mn/TiO_2 for CCl_2F_2 removal. Ogata *et al*. (2007) demonstrated that electrons captured on the TiO_2 catalyst's surface excite active lattice oxygen, which is very useful for oxidizing CCl_2F_2 [16]. According to Dey and Kumar (2020), Mn tends to produce oxides with varying oxidation states, which may affect the characteristics and activity of the catalyst [41]. Through interaction with reducing or oxidant agents, Mn could quickly undergo a reduction-oxidation cycle. Mn with various oxidation states, such as Mn^{+2}, Mn^{+3}, and Mn^{+4}, are common products of the reduction-oxidation reaction. Due to this variation, Mn possesses a great capability to store/release oxygen. According to Putri *et al*. (2022), addition of Mn_3O_4 to TiO_2 would form lattice oxygen species (O_2^-), free oxygen species (O_2), and surface-adsorbed oxygen species (OH^- and $H_2O_{(g)}$). Meanwhile, the oxidation states of Mn^{+2}, Mn^{+3} are a form of tetrahedral and octahedral sites that are important for the reaction because they provide more active sites [47]. Due to these reasons, we believe that the photocatalytic and presence of lattice oxygen with oxidation state on the Mn/TiO_2 would be primarily accountable for the conversion of CCl_2F_2.

As excess oxygen was added into the gas stream, however, the removal efficiency of CCl_2F_2 decreased. These phenomena might be caused by the electronegative property of O_2. In the presence of excess O_2, the electron attachment would occur, resulting in the decrease of CCl_2F_2 conversion. Wang *et al*. (2017) showed that the addition of excess oxygen in the discharge gap led to the electrons being adsorbed by oxygen during the discharge process. The adsorption of electrons could lead to the reduction of electron dissociation [20]. Therefore, we believe that 1% O_2 in the gas stream is sufficient for the effective removal of CCl_2F_2.

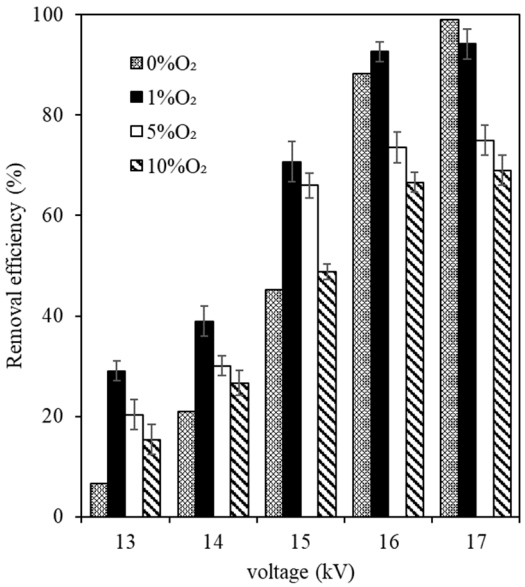

Fig. 2. The influence of voltage and oxygen content on the CCl_2F_2 removal efficiency ($[CCl_2F_2]$ = 800 ppm, Q = 500 sccm, catalyst: Mn/TiO_2, applied voltage ranging from 13 to17 kV, frequency = 15.5 kHz).

In the presence of O_2, it was found that CO_2, N_2O, and $CClF_3$ gas were formed as by-products after removing CCl_2F_2. Wallis *et al*. (2007) also found CO_2, and N_2O as by-products in the decomposition of CCl_2F_2[14]. Chen *et al*. (2021) also reported the formation of CO_x or NO_x in the decomposition of fluorinated

compounds with O_2 in the gas stream. O_2 would generate O species which are useful for oxidizing CCl_2F_2. In the absence of oxygen, O species were generated from the etching of quartz (SiO_2) wall. On the other possibility, O species were generated from the lattice oxygen on Mn/TiO_2 catalyst [21, 22]. Based on Choi *et al*. (2020), etching on plasma only has a rate of 235.5 nm min^{-1} and may not cause considerable damage to the reactor. According to the study, the reaction of fluorocarbon with SiO_2 produced small particles of 5-10 μm, resulting in the un-detected byproducts such as SiF_2 (shown in FTIR result) [50].

The catalyst lifetime is one of the most important parameters for evaluating the catalyst, particularly in terms of the practical application. To investigate the lifetime of catalyst, we carried out the durability test of the catalyst via plasma catalysis for removal of CCl_2F_2. Fig 3 shows the removal efficiency of CCl_2F_2 using DBD system during long-term experiment (~100 hours). The applied voltage was set as 15 kV and the CCl_2F_2 concentration was controlled at 800 ppm. 1 % of O_2 was added with the gas flow rate at 500 sccm. As shown in Fig 3, the removal efficiency of CCl_2F_2 gradually decreased over time. The initial efficiency was 65 % and gradually decreased to 20% after ~100 hours.

The decreasing CCl_2F_2 removal efficiency over time could be attributed to some factors. Firstly, the Mn/TiO_2 catalyst might be the deactivated due to the oxidation of CCl_2F_2. Duan and Henkelman (2018) demonstrated the deactivation of Au/TiO_2 in the presence of O_2 for CO_2 decomposition. It is suggested that high CO_2 binding strength would result in carbonates being adsorbed on active sites of catalysts [23]. Hence, we presume that the presence of carbonates on the active sites of the catalyst could accelerate the deactivation process. Secondly, formation of coke on the catalyst might result in a decreased conversion. Pan *et al*. (2019) reported that formation of coke on the catalyst during the removal of fluorinated compounds would inhibit the performance of the catalyst [24]. As the reaction continues, coke might continuously form and accumulate on the active surface of catalyst. To further investigate the coke formation, we compare (X-Ray Diffraction) XRD profiles between fresh catalyst and used catalyst (reaction in plasma catalysis for ~100 hours).

As shown in Fig. 4 the XRD pattern of the fresh (black line) and used (red line) Mn/TiO_2 catalyst. TiO_2 support is made up of anatase TiO_2 (2θ = 25.3°, 37.8°,48.1°, 53.9°, 55.0°, 62.7°, 68.9° and 70.3°) and traces of rutile TiO_2 (2θ = 37.5° and 58.5°). The characteristic peaks of MnO_2 (2θ = 28.7° and 42.7°) also appeared in the XRD pattern of Mn/TiO_2 [51, 52]. There is no obvious effect on the TiO_2 crystal structure with addition of Mn. However, there is a significant decrease on XRD peak at 2θ = 25.3° after reaction for 100 hours via plasma catalysis. The decrease of XRD peak might indicate a low degree of crystallinity, where the lattice parameter decreased as a function of time. The degree of crystallinity has a great impact on stability, solidity, and sometimes an indication of higher catalytic activity. Žerjav and Pintar (2020) found that decreasing degree of crystallinity in anatase TiO_2 catalyst can also reduce the quality of the photocatalytic activity [54]. Moreover, the formation of coke on the Mn/TiO_2 catalyst surface makes it possible to inhibit the adsorption of UV light. The formation of coke is evidenced by the peak at 2θ = 31.5° in XRD pattern. According to Yang *et al*. (2020), the condition for the appearance of a new peak at 2θ = 31.5° indicates the formation of coke [53]. This formation can be due to the decomposition of carbon contains in CCl_2F_2.

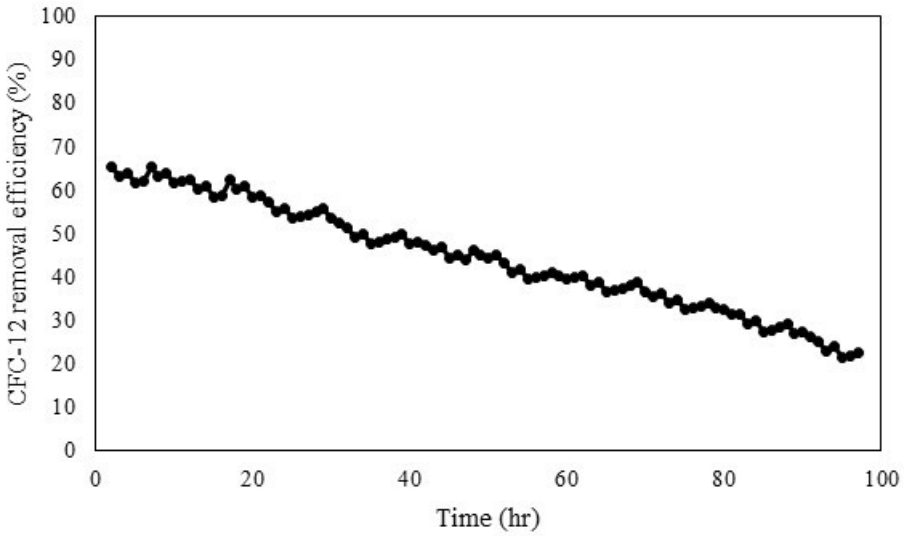

Fig. 3. The change of CCl_2F_2 removal efficiency of plasma system with reaction time. ($[CCl_2F_2]$ = 800 ppm, Q = 500 sccm, $[O_2]$ =1%, catalyst= Mn/TiO_2, applied voltage = 15 kV, frequency= 15.5 kHz).

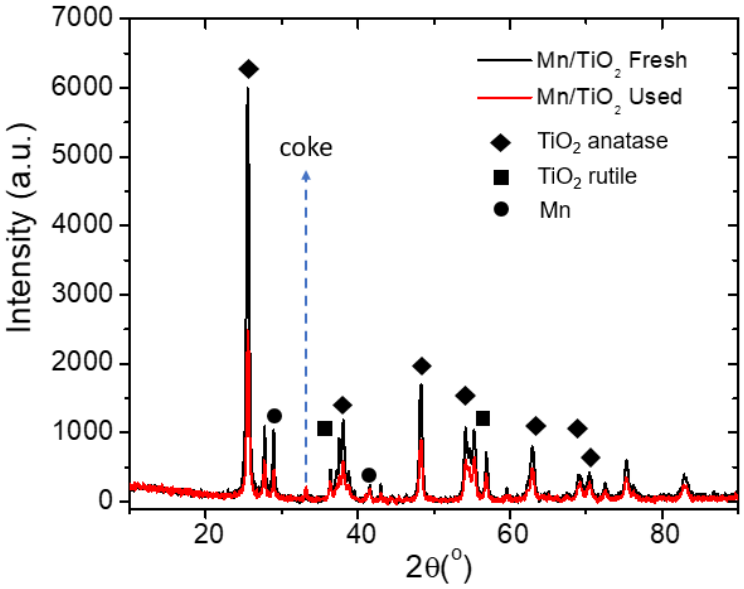

Fig. 4. XRD pattern of Mn/TiO_2 catalyst after 100 h with reaction conditions ([CCl_2F_2] = 800 ppm, Q = 500 sccm, [2] =1%, applied voltage = 15 kV, frequency= 15.5 kHz). XRD patterns of fresh catalyst (black line), XRD of used catalyst (red line) and blue arrow indicate coke formation peak intensity.

3.2 Effect of inlet concentration and gas flow rate on CCl_2F_2 removal

Fig. 5 shows the effect of inlet CCl_2F_2 concentration on the removal efficiency of CCl_2F_2. The system is operated with the applied voltage of 13 -17 kV and the total gas flow rate of 500 sccm. 1% O_2 is also added to the gas stream. The results show that as the inlet CCl_2F_2 concentration increases, its removal efficiency decreases. At the applied voltage of 17 kV, the highest removal efficiency (η = 95 %) was obtained when the inlet CCl_2F_2 concentration was controlled at 800 ppm. At the same applied voltage, the CCl_2F_2 removal efficiency decreased to 32.0% as the inlet CCl_2F_2 concentration was raised to 7,200 ppm.

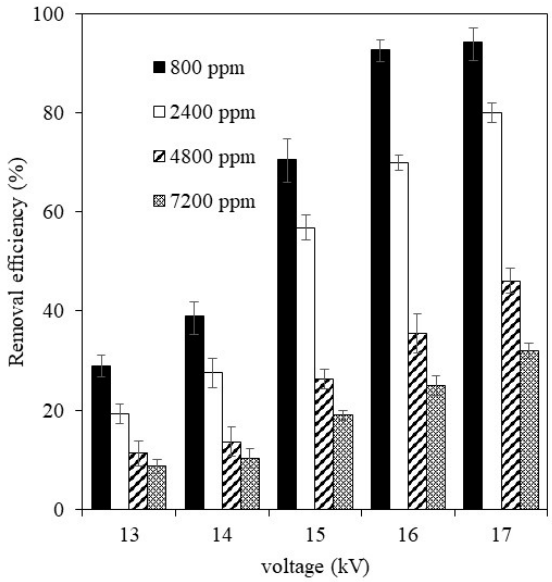

Fig. 5. The effect of CCl_2F_2 concentration and operating voltage on CCl_2F_2 removal efficiency in the presence of oxygen. ([O_2] = 1%, Q = 500 sccm, catalyst: Mn/TiO_2, applied voltage ranging from 13 to17 kV, frequency = 15.5 kHz).

Plasma chemistry involves the number of energetic electrons, photons, positive and negative ions, which are determined by the plasma power. As the applied voltage was increased, more energetic electrons were produced. Eventually, the magnitude of mean electric field would increase as well. The collision of energetic electrons with CCl_2F_2 is considered to be the most important mechanism leading to CCl_2F_2 conversion. As the concentration increases, the interaction between plasma chemistry and catalyst might be limited at constant applied voltage due to excess unreacted CCl_2F_2. As a result, the removal efficiency of CCl_2F_2 decreases.

To further investigate the effect of CCl_2F_2 concentration, we observe the removal rate of CCl_2F_2 at various applied voltages. As shown in Fig. 6, increasing inlet CCl_2F_2 concentration would increase its removal rate, although the removal efficiency of CCl_2F_2 decreased with increasing inlet CCl_2F_2 concentration. The removal rate of CCl_2F_2 with the inlet concentration of 7200 ppm and applied voltage of 17 kV reached 342.0 mg h^{-1} while the CCl_2F_2 removal efficiency was reduced to less than 35% (see Fig. 5). This kind of discrepancy could be explained by Equation 2, as the removal rate is proportional to the efficiency and concentration of CCl_2F_2. As the inlet CCl_2F_2 concentration increases, the removal rate of CCl_2F_2 should increase as long as the reducing level of CCl_2F_2 removal efficiency is lower than the increasing level of inlet CCl_2F_2 concentration.

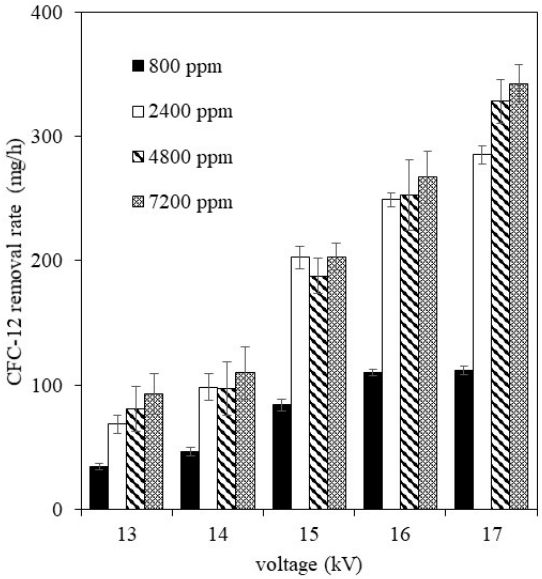

Fig. 6. The effect of CCl_2F_2 concentration and applied voltage on CCl_2F_2 removal rate in the presence of oxygen. ($[O_2]$ = 1%, Q = 500 sccm, catalyst: Mn/TiO_2, applied voltage ranging from 13 to17 kV, frequency = 15.5 kHz).

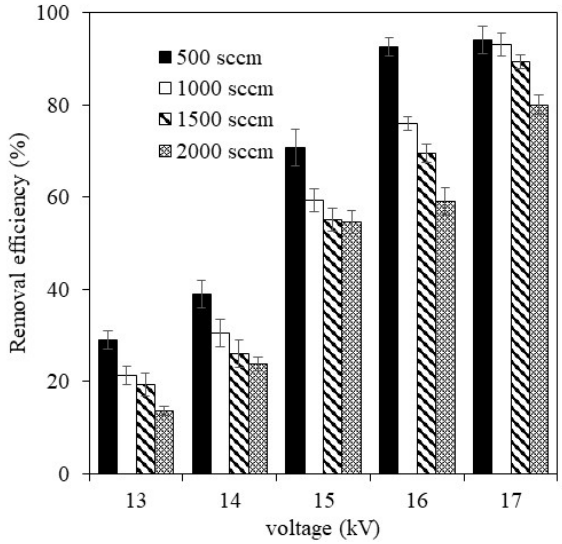

Fig. 7. The effects of gas flow rate and applied voltage on the CCl_2F_2 removal efficiency. ($[CCl_2F_2]$ = 800 ppm, $[O_2]$ = 1% catalyst: Mn/TiO_2, applied voltage ranging from 13 to17 kV, frequency = 15.5 kHz).

To further understand the effect of gas flow rate on the removal efficiency of CCl_2F_2, the gas streams with varying gas flow rates were generated for tests. Fig. 7 shows the changes in CCl_2F_2 removal efficiency with varying gas flow rates within the range of 500-2000 sccm. The gas streams with 800 ppm CCl_2F_2 and 1% O_2 were experimentally tested. The results show that at same applied voltage, the removal efficiency of CCl_2F_2 decreased as the flow rate increased. At 17 kV, the CCl_2F_2 removal efficiency reached 94.2% as the total gas flow was controlled at 500 sccm. At the same voltage, the removal efficiency of CCl_2F_2 reduced to 80.0% as the total flow rate of the system was increased to 2000 sccm. The decreasing removal efficiency is associated with the residence time of the gas inside the reactor. As the gas flow rate decreased, the residence time of the gas in the reactor increased. Due to the increasing gas residence time, the gas molecules would accept more energy through the discharge region. Therefore, it could enhance the internal energy of CCl_2F_2 molecules and promote the removal efficiency.

3.3 Removal mechanism and byproducts

Fig. 8 shows the FTIR spectra of CCl_2F_2 before discharge (Fig. 8a) and after discharge (Fig. 8b). As shown in Fig. 8a, the CCl_2F_2 spectra consist of two regions of absorbance at 850 cm^{-1} and 1060-1180 cm^{-1}, respectively. Before discharge, the by-products were not detected because CCl_2F_2 was not decomposed yet. After discharge, we could see several spectra at 850 to 1060-1180, 1250-1400, 1560-1650, 1780-1850, 2150-2260, and 2300-2400 cm^{-1} which represent the existence of $CClF_3$, N_2O, NO_2, NOCl, N_2O and CO_2, respectively.

The initial stage in plasma chemistry is to generate energetic electrons to dissociate molecules in the gas stream such as nitrogen, oxygen, and CCl_2F_2. On the other hand, molecules from the gas stream will be adsorbed and broken down by high-energy electrons, resulting in active substances like ground-state oxygen, nitrogen atoms, or molecules excited by electrons ($O^*(^3P, ^1D)$, $O_2(a^1\Delta)$, O^3, $N^*(^4S, ^2D, ^2P)$, $N_2(A^3\sum_u^+)$) please see process one and process three (P1 and P3) [25–26]. Sierra *et al*. (2004) discovered that electron impact ionization in CCl_2F_2 results in the formation of CCl^+; $CClF^+$; $CClF_2^+$; $CClF_2^{2+}$; $CClF_3^+$; CF^+; CF_2^+; CF_3^+; Cl^+ and F^+ please see process one and process three (P1 and P3). N_2 radical species such as $N_2(A^3\sum_u^+)$ help break C–Cl or C–F bonds, as demonstrated in R3 [27]. At the same time, UV light ($300 < \lambda < 380$ nm) from plasma chemistry can generate a photocatalysis process to form lattice oxygen to further oxidize CCl_2F_2 please see process two and process four (P2 and P4) [49]. CCl_2F_2 initially combines with oxygen atoms from gas streams, oxygen radicals from photocatalysts, and possibly electron impact dissociation to create COF_2, ClO, CO, and CO_2 and desorption as by product, please see process three and process five (P3 and P5). The C–Cl link in CF_2Cl_2 is weaker than the C–F bond, CF_2Cl and Cl are formed in these two circumstances. The CF_2Cl_2 molecule has a higher dissociative electron attachment cross section, which can promote dissociative electron attachment during the removal of CCl_2F_2. As illustrated in Reactions 4-8, CF_2Cl radicals react with O_2 to create peroxyl radicals, which are then transformed into COF_2, ClO, CO, and CO_2. According to Herron (1999) and Umemoto *et al*. (2000), N_2 $A^3\sum_u^+$, $N(^2D)$, $N(^2P)$, and $N(^4S)$ have high CF_4 decomposition potential (see Reactions 9-12) [28, 30]. Harling *et al*. (2005) demonstrated that reactive nitrogen species react with ClO to form NCl molecules, which then react with ClO to form NOCl [29]. Furthermore, NO may combine with Cl_2 to form NOCl. Reaction 13-16 illustrates the various methods for producing NOCl please see process three and process five (P3 and P5) [31, 37-40]. Simultaneously, NO_2 and N_2O would arise as undesired by-products since the excited nitrogen atom combines with molecular oxygen to generate NO or N_2O please see process three and process five (P3 and P5) [14]. However, atomic oxygen or ozone will further oxidize NO to create NO_2. Additionally, TiO_2 can decompose N_2O or NO_2, even though unwanted by-products can still develop [42]. This phenomenon occurs due to the competition among CCl_2F_2, N_2O, and NO_x on the catalyst surface. Further studies need to be conducted to develop catalysts that reduce the generation of unwanted by-products such as N_2O and NO_x.

The second possibility is the presence of Mn/TiO_2 catalyst in the CCl_2F_2 oxidation process. Mn/TiO_2 donates oxygen through the oxygen lattice produced in the photocatalytic process. The basic photocatalytic process's concept can be clarified using TiO_2 as a catalyst. The first step starts with TiO_2 to capture protons from plasma chemistry, whose energy is greater than its band gap (3.2 eV for anatase and 3.0 eV for rutile), the photoinduced electrons are excited to the conduction band, leaving positive holes on the valence band, and thus creating the electron-hole pairs [46]. Furthermore, some of them recombine with each other to release heat or emit light, others would transfer to the surface of the catalyst and participate in surface chemical reactions.

However, addition of Mn to TiO_2 can improve the photocatalytic process. As described by Fu *et al*. (2021), suggesting that Mn^{4+} can boost the catalytic photoactivity process due to the presence of Mn^{4+} electrons that were photoexcited in rutile migrate to the conduction band of anatase, thereby effectively suppressing the recombination. Moreover, doping manganese ions such as Mn 3d and the carbon layer formed in the calcination process can reduce the band gap energy and promote photocatalytic activity both in terms of absorption and easier charge-discharge [19]. Bharati *et al*. (2020) report that there are enhancements in the concentration of oxygen vacancies by doping Mn into TiO_2 detected through XPS. Moreover, the addition of Mn also gives the effect of the existence of Mn in different oxidation states such as Mn^{4+}, Mn^{3+}, and Mn^{2+}. This state can significantly evoke the formation of the anatase phase. In summary, the presence of Mn in TiO_2 has a major effect on the formation of oxygen lattice which affects the oxidation of CCl_2F_2 [52].

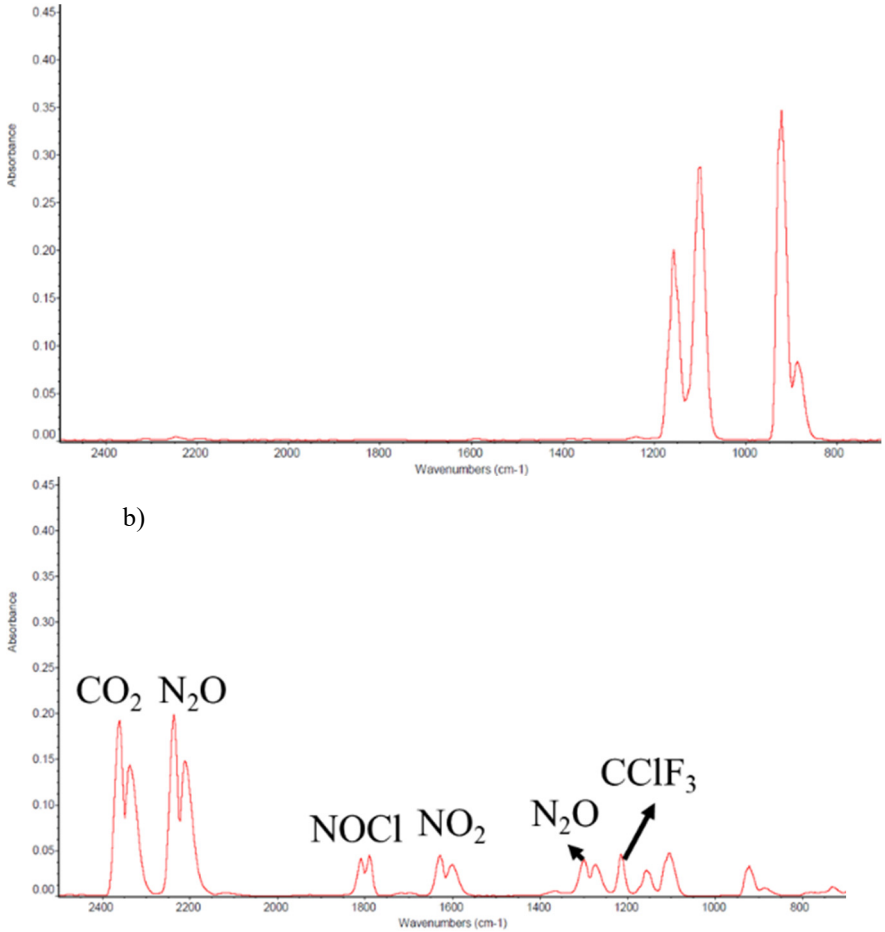

Fig. 8. CCl_2F_2 FTIR spectra: a) before discharge, b) after discharge. ([CCl_2F_2] = 800 ppm, Q = 500 sccm, [O_2] = 1%, catalyst = Mn/TiO_2, applied voltage 15 kV, frequency = 15.5 kHz).

$$N_2(A^3\textstyle\sum_u^+) + CF_2Cl_2 \rightarrow CF_2Cl + Cl \qquad k_{25°C} = 1.50 \times 10^{-13} \qquad (3)$$

$$O(^1D) + CF_2Cl_2 \rightarrow \cdot CClF_2 + ClO \qquad k_{25°C} > 0.40 \qquad (4)$$

$$\cdot CClF_2 + O_3 \rightarrow O_2 + CF_2ClO \qquad k_{25°C} > 1.00 \times 10^{-14} \qquad (5)$$

$$O_3 + \cdot Cl \rightarrow O_2 + ClO \qquad k_{25°C} = 1.84 \times 10^{-11} \qquad (6)$$

$$CF_2ClO \rightarrow COF_2 + \cdot Cl \qquad k_{25°C} = 7.53 \times 10^{-5\,*} \qquad (7)$$

$$O(^1D) + COF_2 \rightarrow CO_2 + F_2 \qquad k_{25°C} = 2.19 \times 10^{-11} \qquad (8)$$

$$N(^2D) + CF_4 \rightarrow \text{Products} \qquad k_{25°C} = 1.0 \times 10^{-13} \qquad (9)$$

$$N(^4S) + CF_4 \rightarrow \text{Products} \qquad k_{25°C} = 2.68 \times 10^{-10} \qquad (10)$$

$$N_2\ A^3\textstyle\sum_u^+ + CF_4 \rightarrow \text{Products} \qquad k_{25°C} = 1.0 \times 10^{-14} \qquad (11)$$

$$N(^2P) + C_2F_4 \rightarrow \text{Products} \qquad k_{25°C} = 2.4 \times 10^{-11} \qquad (12)$$

$$ClO + N \rightarrow NO + \cdot Cl \qquad k_{25°C} < 4.98 \times 10^{-14} \qquad (13)$$

$$ClOO + NO \rightarrow NOCl + O_2 \qquad k_{25°C} = 11^* \qquad (14)$$

$$NO + \cdot Cl \rightarrow NOCl \qquad k_{25°C} = 8.92 \times 10^{-32} \qquad (15)$$

$$NCl + ClO \rightarrow NOCl + \cdot Cl \qquad k_{25°C} = 2.31 \times 10^{-11} \qquad (16)$$

(* mark stands for first order reaction (s^{-1}))

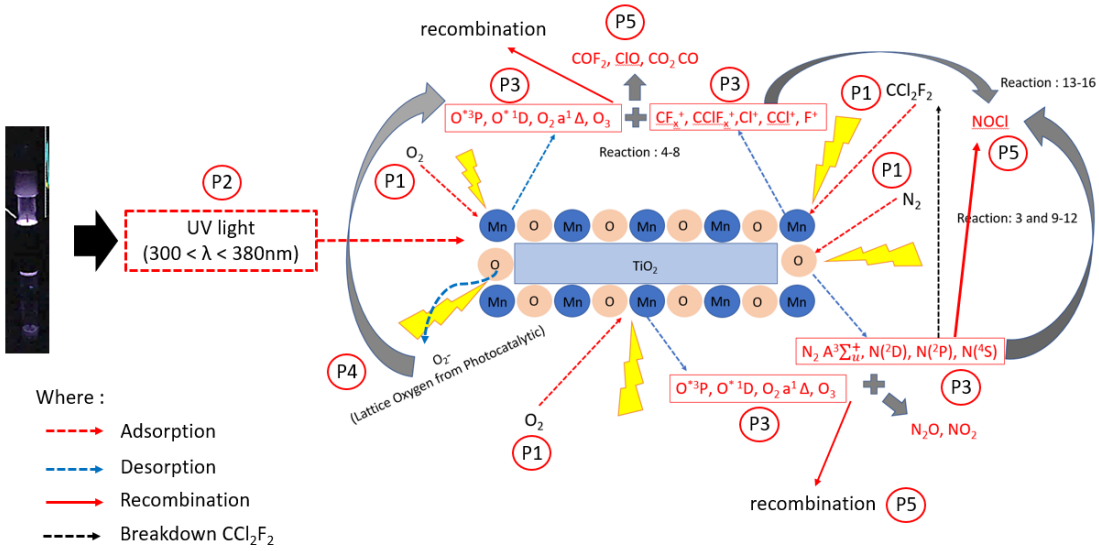

Fig. 9. Proposed schematic of the reaction pathways for removal of CCl_2F_2 in nitrogen plasma with Mn/TiO_2 catalyst and 1% O_2.

4. Conclusion

The DBD plasma is integrated with Mn/TiO_2 to form plasma catalysis system which greatly improves the removal efficiency of CCl_2F_2. The highest removal efficiency of CCl_2F_2 achieved is 99.0%. In terms of the influence of operating parameters in the plasma catalysis system, the CCl_2F_2 removal efficiency achieved is positively correlated with the operating voltage. CCl_2F_2 removal efficiency is optimum at addition of 1% of oxygen. On the other hand, CCl_2F_2 removal efficiency is negatively correlated with excess oxygen content, as well as CCl_2F_2 concentration and gas flow rate. The products including CO_2, N_2O, NO_X, NOCl and $CClF_3$ are detected for the gas stream containing 1% O_2, 800 ppm CCl_2F_2. Moreover, CCl_2F_2 has a large dissociative electron reaction cross section and is easy to react with high-energy electrons. Hence, the removal mechanism is the decomposition via the reactions with $N_2(A^3\sum_u^+)$, $N^*(^4S, ^2D, ^2P)$ and high-energy electrons generated by plasma. On the other hand, the integration effect between plasma and catalyst is a decisive factor in the removal of CCl_2F_2. The addition of Mn into TiO_2 can increase the photocatalytic process which is very useful for the removal of CCl_2F_2. On the other hand, catalyst deactivation is one of the disadvantages of using Mn/TiO_2 as shown in the durability test and further investigation is required to prevent the catalyst deactivation for the removal of CCl_2F_2.

Acknowledgment

Authors would like to express their gratitude to the Industrial Technology Research Institute for funding.

References

[1] United Nations Environment Programme, Ozone secretariat : Handbook for the montreal protocol on substances that deplete the ozone layer. UNEP/Earthprint, 2006.
[2] Dincer, I., Refrigeration systems and applications. John Wiley & Sons, 2017.
[3] McCulloch A., Ashford P., and Midgley P.M., Historic emissions of fluorotrichloromethane (CFC-11) based on a market survey, *Atmos. Environ*., Vol. 35 (26), pp. 4387–4397, 2001.
[4] McCulloch A., Midgley P.M., and Ashford P., Releases of refrigerant gases (CFC-12, HCFC-22 and HFC-134a) to the atmosphere, *Atmos. Environ*., Vol. 37 (7), pp. 889–902, 2003.
[5] Advanced Global Atmospheric Gases Experiment, Research and assessment program. Retrieved from https://agage.mit.edu/data/afeas-data, 2006.
[6] Intergovernmental Panel on Climate Change, Fifth assesment report. Retrieved from https://www.ipcc.ch/assessment-report/ar5/, 2014.
[7] Rowland F.S., and Molina M.J., Chlorofluoromethanes in the environment, *Rev. Geophys*., Vol. 13 (1), pp. 1–35, 1975.
[8] Ueno H., Iwasaki Y., Tatsuichi S., and Soufuku M., Destruction of chlorofluorocarbons in a cement kiln, *J. Air Waste Manag. Assoc*., Vol. 47 (11), pp. 1220–1223, 1997.
[9] Wang Y.F., Lee W.J., Chen C.Y., and Hsieh L.T., Decomposition of dichlorodifluoromethane by adding hydrogen in a cold plasma system, *Environ. Sci. Technol*., Vol. 33 (13), pp. 2234–2240, 1999.
[10] Bonarowska M., Burda B., Juszczyk W., Pielaszek J., Kowalczyk Z., and Karpi Z., Hydrodechlorination of CCl_2F_2 (CFC-12) over Pd-Au/C catalysts, *Applied Catalysis B Environmental.*, Vol. 35 (1), pp. 13–20, 2001.
[11] Kim H.H., Abdelaziz A.A., Teramoto Y., Nozaki T., Hensel K., Mok., Y.S., Saud S., Nguyen D.B., Lee D.H., and Kang W.S., Interim report of plasma catalysis: Footprints in the past and blueprints for the future, *Int. J. Plasma Environ. Sci. Technol*., Vol. 15 (1), e01004, 2021.
[12] Kim H.H., Ogata A., and Futamura S., Complete oxidation of volatile organic compounds (VOCs) using plasma-driven catalytic and oxygen plasma, *Int. J. Plasma Environ. Sci. Technol*., Vol. 1 (1), pp. 46–51, 2007.
[13] Kim H. H., and Ogata A., Interaction of nonthermal plasma with catalyst for the air pollution control, *Int. J. Plasma Environ. Sci. Technol*., Vol. 6 (1), pp. 43–48, 2012.
[14] Wallis A., Whitehead J., and Zhang K., Plasma-assisted catalysis for the destruction of CFC-12 in atmospheric pressure gas streams using TiO_2, *Catal. Lett.*, Vol. 113, pp. 29–33, 2007.
[15] Ren G., Jia L., Zhao G, Zhou T., Yang X., Li R., Chang Y., and Liu T ., Catalytic decomposition of dichlorodifluoromethane (CFC-12) over MgO/ZrO_2 solid base catalyst, *Catal. Lett..,* Vol. 149 (2), pp. 507–512, 2019.
[16] Ogata A., Kim H.H., Oh S.M., and Futamura S., Evidence for direct activation of solid surface by plasma discharge on CFC decomposition, *Thin Solid Films.*, Vol. 506, pp. 373–377, 2006.
[17] Kiricsi I., and Nagy J. B., Surface intermediates generated in the decomposition of C1 chlorofluorocarbons over oxides and zeolites of acid-base and redox character, *Appl. Catal. A Gen*., Vol. 271 (1–2), pp. 27–38, 2004.
[18] Parrino F., and Palmisano L., Titanium dioxide (TiO_2) and its Applications, *Metal Oxide Series, Elsevier.*, 2021.
[19] Fu F., Zhang Y., Zhang Y., and Chen Y., Synthesis of Mn-doped and anatase/rutile mixed-phase TiO_2 nanofibers for high photoactivity performance, *Catal. Sci. Technol.*, Vol. 11 (12), pp. 81–95, 2021.
[20] Wang J., Yi H., Tang X., Zhao S., Gao F., Zhang R., & Yang Z., Products yield and energy efficiency of dielectric barrier discharge for NO conversion: Effect of O_2 content, NO concentration, and flow rate, *Energy Fuels.*, Vol. 31 (9), pp. 9675–9683, 2017.
[21] Chen Y.S., Pan K.L., Machmud A., and Chang M.B., Integration of plasma with catalyst for removing CF_4 from gas streams, *Int. J. Plasma Environ. Sci. Technol*., Vol. 15 (3), e03004, 2021.
[22] Manceau A., Marcus M.A., and Grangeon S., Determination of Mn valence states in mixed-valent manganates by XANES spectroscopy, *Am. Mineral*., Vol. 97 (5–6) pp. 816–827, 2012.
[23] Duan Z., and Henkelman G., Calculations of CO oxidation over a Au/TiO_2 catalyst: A study of active sites, catalyst deactivation, and moisture effects, *ACS Catal*., Vol. 8 (2), pp. 1376–1383, 2018.
[24] Pan K.L., Chen Y.S., and Chang M.B., Effective removal of CF_4 by combining nonthermal plasma with γ-Al_2O_3, *Plasma Chem. Plasma Process*., Vol. 39 (4), pp. 877–896, 2019.
[25] Herron J. T., Modeling studies of the formation and destruction of NO in pulsed barrier discharges in nitrogen and air, *Plasma Chem. Plasma Process*., Vol. 21 (4), pp. 581–609, 2001.
[26] Kim D.J., Choi Y., and Kim K.S., Effects of process variables on NO_x conversion by pulsed corona discharge process,

Plasma Chem. Plasma Process., Vol. 21 (4), pp. 625–650, 2001.
[27] Sierra B., Martínez R., Redondo C., and Castaño F., Electron-impact ionisation cross-sections of the $CClF_3$ and CCl_3F molecules, *Int. J. Mass Spectrom*., Vol. 235 (3), pp. 223–228, 2004.
[28] Herron J. T., Evaluated chemical kinetics data for reactions of $N(^2D)$, $N(^2P)$, and $N_2(A^3\Sigma_u^+)$ in the gas phase, *J. Phys. Chem. Ref. Data.*, Vol. 28 (5), pp. 1453–1483, 1999.
[29] Harling A.M., Whitehead J.C., and Zhang K., NO_x formation in the plasma treatment of halomethanes, *J. Phys. Chem. A*., Vol. 109 (49), pp. 11255–11260, 2005.
[30] Umemoto H., Terada N., Tanaka K., and Oguro S., Deactivation processes of highly excited atomic nitrogen, $N(2p^23p^2S)$, *Phys. Chem. Chem. Phys*., Vol. 2, pp. 3425–3428, 2000.
[31] Beckham L.J., Fessler W.A., and Kise M.A., Nitrosyl chloride, *Chem. Rev*., Vol. 48 (3), pp. 319–396, 1951.
[32] Gillespie H.M., and Donovan R.J., Reaction of $O(2^1D_2)$ atoms with chlorofluoromethanes: formation of ClO, *Chem. Phys. Lett*., Vol. 37 (3), pp. 468–470, 1976.
[33] Ralph D.G., and Wayne R.P., Reactions of the chlorodifluoromethyl radical formed in the photolysis of halogenocarbon + ozone mixtures*, J. Chem. Soc. Faraday Trans*., Vol. 78 (11), pp. 1815–1823, 1982.
[34] Freeman C.G., and Phillips L.F., Kinetics of chlorine oxide reactions. II. The reaction of nitrogen atoms with Cl_2O [chlorine oxide], *J. Phys. Chem*., Vol. 72 (8), pp. 3028–3030, 1968.
[35] Clyne M.A.A., and Watson R.T., Kinetic studies of diatomic free radicals using mass spectrometry. Part 2.—Rapid bimolecular reactions involving the ClO $X^2\Pi$radical, *J. Chem. Soc. Faraday Trans*., Vol. 70, pp. 2250–2259, 1974.
[36] Atkinson R., Baulch D.L., Cox R.A., Jr R.F.H., Kerr J.A., and Troe J., Evaluated kinetic and photochemical data for atmospheric chemistry: Supplement IV. IUPAC subcommittee on gas kinetic data evaluation for atmospheric chemistry, *J. Phys. Chem. Ref. Data*., Vol. 21 (6), pp. 1125–1568, 1992.
[37] Atkinson R., Baulch D.L., Cox R.A., Jr R.F.H., Kerr J.A., Rossi M.J., and Troe J., Evaluated kinetic, photochemical and heterogeneous data for atmospheric chemistry: Supplement V. IUPAC subcommittee on gas kinetic data evaluation for atmospheric chemistry, *J. Phys. Chem. Ref. Data*., Vol. 26 (3), pp. 521–1011, 1997.
[38] Wongdontri S.W., Simonaitis R., and Heicklen J., The reaction of ClOO with NO, *Geophys. Res. Lett.,* Vol. 5 (12), pp. 1005–1008, 1978.
[39] DeMore W.B., Margitan J.J., Molina M.J., Watson R.T., Golden D.M., Hampson R.F., Kurylo M.J., Howard C.J., Ravishankara A.R., Kolb C.E., and Molina M.J., Chemical kinetics and photochemical data for use in stratospheric modeling, Evaluation number 12. *JPL Publication*., Vol. 97–4, 1997.
[40] Clyne M.A.A., MacRobert A.J., and Stief L.J., Elementary reactions of the NCl radical. Part 2.—Kinetics of the NCl + ClO and NCl + NO reactions, *J. Chem. Soc. Faraday Trans.,* Vol. 81 (1), pp. 159–167, 1985.
[41] Dey S., and Kumar V.P., The performance of highly active manganese oxide catalysts for ambient conditions carbon monoxide oxidation, *Curr. Opin. Green Sustain. Chem.,* Vol. 3, 100012, 2020.
[42] Kočí K., Reli M., Troppová I., Šihor M., Kupková J., Kustrowski P., and Praus P., Photocatalytic decomposition of N_2O over TiO_2/g-C_3N_4 photocatalysts heterojunction, *Appl. Surf. Sci*., Vol. 396 (1), pp. 1685–1695, 2017.
[43] Chen Y.S., Pan K.L., and Chang M.B., Application of plasma catalysis system for C_4F_8 removal, *Environ. Sci. Pollut. Res.*, Vol. 28 (41), pp. 57619–57628, 2021.
[44] Azadmanjiri J., Berndt C.C., Wang J., Kapoor A., Srivastava V.K., and Wen C., A review on hybrid nanolaminate materials synthesized by deposition techniques for energy storage applications, *J. Mater. Chem. A.*, Vol. 2 (11), pp. 3695–3708, 2014.
[45] Zhang Y.R., Neyts E.C., and Bogaerts A., Influence of the material dielectric constant on plasma generation inside catalyst pores, *J. Phys. Chem. C.*, Vol. 120 (45), pp. 25923–25934, 2016.
[46] Zhao X., Zhang G., and Zhang Z., TiO_2-based catalysts for photocatalytic reduction of aqueous oxyanions: State-of-the-art and future prospects, *Environ Int*., Vol. 136, 105453, 2020.
[47] Putri R.A.K., Nashrah N., Han D.I., Al Zoubi W., and Ko Y.G., Chemical incorporation of Mn_3O_4 into TiO_2 coating by benzotriazole working as electron donor: Electrochemical and catalytic performance, *Compos. B: Eng*., Vol. 232, pp. 109609, 2022.
[48] Li D., Xu K., Niu Z., and Zhang C., Annealing and plasma effects on the structural and photocatalytic properties of TiO_2 fibers produced by electrospinning, *Catalysts*., Vol. 12 (11), 1441, 2022.
[49] Sano T., Negishi N., Sakai E., and Matsuzawa, S., Contributions of photocatalytic/catalytic activities of TiO_2 and γ-Al_2O_3 in nonthermal plasma on oxidation of acetaldehyde and CO. *J Mol Catal A Chem.*, Vol. 245 (1-2), pp. 235–241, 2006.
[50] Choi, J.H., Yoon, J., Jung, Y., Min, K. W., Im, W. B., and Kim, H.J., Analysis of plasma etching resistance for commercial quartz glasses used in semiconductor apparatus in fluorocarbon plasma. *Mater. Chem. Phys*., Vol. 272, 125015, 2021.
[51] Li, W., Liang, R., Hu, A., Huang, Z., and Zhou, Y. N., Generation of oxygen vacancies in visible light activated one-dimensional iodine TiO_2 photocatalysts. *RSC Adv*., Vol. 4 (70), pp. 36959–36966, 2014.
[52] Bharati, B., Mishra, N. C., Sinha, A. S. K., and Rath, C., Unusual structural transformation and photocatalytic activity of Mn doped TiO_2 nanoparticles under sunlight. *Mater. Res. Bull*., Vol. 123, pp. 110710, 2020.

[53] Yang, L., Yao, L., Jiang, W., Jiang, X., and Li, J., The study on continuous denitrification, desulfurization of pyrolusite/activated coke hybrid catalyst. *RSC Adv*., Vol. 8 (1), pp. 406–413, 2018.
[54] Žerjav, G., and Pintar, A. Influence of TiO_2 morphology and crystallinity on visible-light photocatalytic activity of TiO_2-Bi_2O_3 composite in AOPs. *Catalysts.*, Vol. 10 (4), 395, 2020.
[55] Kim, H.H., Teramoto, Y., Ogata, A., Takagi, H., and Nanba, T. Plasma catalysis for environmental treatment and energy applications. *Plasma Chem. Plasma Process*., Vol. 36 (1), pp. 45–72, 2016.
[56] KP Veerapandian, S., De Geyter, N., Giraudon, J.M., Lamonier, J.F., and Morent, R. The use of zeolites for VOCs abatement by combining non-thermal plasma, adsorption, and/or catalysis: a review. *Catalysts*, Vol. 9 (1), 98, 2019.